Psychiatry Research: Neuroimaging 260 (2017) 53–61

Contents lists available at ScienceDirect

Psychiatry Research Neuroimaging

journal homepage: www.elsevier.com/locate/psychresns

Cerebral blood flow and its connectivity features of auditory verbal hallucinations in schizophrenia: A perfusion study

Long-Biao Cui[a,1], Gang Chen[a,b,1], Zi-Liang Xu[c,1], Lin Liu[c], Hua-Ning Wang[d], Li Guo[d], Wen-Ming Liu[d], Ting-Ting Liu[a], Shun Qi[a], Kang Liu[a], Wei Qin[c], Jin-Bo Sun[c], Yi-Bin Xi[a,*], Hong Yin[a,*]

[a] Department of Radiology, Xijing Hospital, Fourth Military Medical University, Xi'an, Shaanxi, China
[b] Department of Radiology, General Hospital of Lanzhou Military Region, Lanzhou, China
[c] School of Life Sciences and Technology, Xidian University, Xi'an, Shaanxi, China
[d] Department of Psychiatry, Xijing Hospital, Fourth Military Medical University, Xi'an, Shaanxi, China

ARTICLE INFO

Keywords:
Schizophrenia
Auditory verbal hallucinations
Arterial spin labeling
Cerebral blood flow
Language processing

ABSTRACT

The goal of the study was to investigate cerebral blood flow (CBF) and its connectivity (an across-subject covariance measure) patterns of schizophrenia (SZ) patients with auditory verbal hallucinations (AVHs). A total of demographically matched 25 SZ patients with AVHs, 25 without AVHs, and 25 healthy controls (HCs) underwent resting state perfusion imaging using a pulsed arterial spin labeling sequence. CBF and its connectivity were analyzed and then CBF topological properties were calculated. AVHs patients exhibited decreased CBF in the bilateral superior and middle frontal gyri and postcentral gyri, and right supplementary motor area compared with SZ patients without AVHs. SZ patients without AVHs showed reduced CBF in the left middle frontal gyrus relative to HCs. Moreover, AVHs groups showed distinct connectivity pattern, an intermediate level between HCs and patients without AVHs in the global efficiency. Our study demonstrates aberrant CBF in the brain regions associated with inner speech monitoring and language processing in SZ patients with AVHs. The complex network measures showed by CBF-derived functional connectivity indicate dysconnectivity between different functional units within the network of AVHs in SZ. Our findings might shed light on the neural underpinnings behind AVHs in this devastating disease at the level of CBF and its connectivity.

1. Introduction

As one of the leading causes of health burden in the world, schizophrenia (SZ) is a severe and complex psychiatric disorder, with a global prevalence of around 1% (APA, 2013; Whiteford et al., 2013). Auditory verbal hallucinations (AVHs), one of featured and debilitating symptoms in SZ, are liable to become chronic and resistant to medication (Shergill et al., 1998). Elucidation of neural mechanisms behind AVHs in SZ is of great clinical significance for diagnosis and treatment of this debilitating mental disease.

Symptom-based research has provided provisional insights into the altered brain regions and networks involving AVHs in SZ due to advances of modern functional neuroimaging methods for years (Chang et al., 2015; Cui et al., 2016; Huang et al., 2015; Lennox et al., 2000; Seok et al., 2007; Shin et al., 2005). A systematic review by Upthegrove et al. shows that functional neuroimaging studies focus on the regional and global functions of auditory networks in AVHs (Upthegrove et al., 2016). Blood oxygen level-dependent (BOLD)-functional magnetic resonance imaging (fMRI), which is correlated with local field spontaneous neural activity thereby being considered to be biologically or physiologically significant (Logothetis et al., 2001), not only enables us to evaluate regional brain function but also allows the investigation of functional connectivity (FC) in brain networks. However, BOLD signal tends to be influenced by multiple physiological factors, including cerebral blood flow (CBF), cerebral blood volume, and cerebral metabolic rate of oxygen. As another biomarker of regional brain function, CBF with a more definite physiological implication is usually tightly coupled to brain metabolism and its quantification is allowed by arterial spin labeling (ASL) (Raichle, 1998).

By means of ASL, recent in vivo studies have been used to disclose the pathophysiology of several neuro/psychopathology, including frontotemporal lobar degeneration, Alzheimer disease (AD), and SZ (Du et al., 2006; Hu et al., 2010; Zhu et al., 2015). ASL has also been

* Corresponding authors at: Department of Radiology, Xijing Hospital, Fourth Military Medical University, No. 127 West Changle Road, Xi'an, Shaanxi 710032, China
E-mail addresses: xyb1113@qq.com (Y.-B. Xi), yinhong@fmmu.edu.cn (H. Yin).
[1] These authors contributed equally to this work.

http://dx.doi.org/10.1016/j.pscychresns.2016.12.006
Received 2 August 2016; Received in revised form 7 December 2016; Accepted 10 December 2016
Available online 11 December 2016
0925-4927/

successfully used to measure the decrease in CBF of frontal and temporal regions involving the left auditory cortex and Broca's area in SZ patients with AVHs who had an excellent clinical response to transcranial direct current stimulation (tDCS) or transcranial magnetic stimulation (TMS) (Homan et al., 2011; Kindler et al., 2013). More importantly, the regional CBF among different brain regions are not isolated. The highest concurrent fluctuations in CBF have been identified between homologous cortical regions, and the functional network constructed by CBF connectivity exhibits similar network properties to the networks constructed by anatomical or functional connectivity (Melie-Garcia et al., 2013). Recently, using a group-level independent component analysis on ASL-CBF data, Kindler et al. have found increased CBF connectivity within the default-mode network (DMN) in SZ (Kindler et al., 2015).

We have previously reported that AVHs in SZ involve the dysfunction of auditory-language processing and information filtering brain regions (Chang et al., 2015; Cui et al., 2016; Huang et al., 2015). However, CBF and its connectivity in language/auditory/information filtering-related regions of SZ patients with AVHs are still not well understood despite disturbed functional connectivity detected in SZ patients with AVHs using BOLD-fMRI (Clos et al., 2014; Hoffman et al., 2011; Kawaguchi et al., 2005; Lawrie et al., 2002; Sommer et al., 2012). We hypothesize that AVHs in SZ are associated with abnormal connectivity between auditory-language processing and information filtering brain regions as measured with CBF. In the present study, we used ASL to investigate SZ patients with and without AVHs during resting state from the perspective of both CBF and its connectivity, thereby providing a better understanding of the pathophysiological correlates of AVHs in SZ.

2. Subjects and methods

2.1. Subjects

This study was approved by the ethical committee of our institution, and all participants provided written informed consent after complete description of the study. A total of demographically matched 25 SZ patients with AVHs, 25 without AVHs, and 25 healthy controls (HCs) were included in the case-control observational study (Table 1). In the current study, there were a few overlapping subjects used in our previous study (Chang et al., 2015), but different MRI data were analyzed. Subjects from our outpatient clinic were assessed according to the Diagnostic and Statistical Manual of Mental Disorders, Fourth Edition, Text Revision (DSM-IV-TR) criteria and consensus diagnoses of SZ were made using all the available information. This was based on the scores of the Positive And Negative Syndrome Scale (PANSS) (score ≥60) at the time of scanning (Kay et al., 1987). Other inclusion criteria were that subjects were right handed and their biological parents were Chinese Han population. Patients with AVHs were those who reported AVHs at least once a day for the past four weeks, and the severity of AVHs was assessed by the Auditory Hallucination Rating Scale (AHRS) (Hoffman et al., 2003). Subjects who had never experienced AVHs or had not within the past two years were assigned to patients without AVHs (Non-AVHs) group. The following exclusion criteria applied to all groups: another axis I or II psychiatric disorder, history of significant neurological or systematic illness, diagnosis of substance abuse in the prior 30 days or substance dependence in the prior 6 months, pregnancy or MRI contraindications (i.e., cardiac pacemakers and other metallic implants), intervention using TMS, tDCS, electroconvulsive therapy (ECT) or behavioral therapy, and head motion of > 3 mm translation and/or 3.0° rotation during scanning with consideration of its potential confounding effect (Van Dijk et al., 2012; Zeng et al., 2014b). AVHs and Non-AVHs groups contained both first-episode drug-naïve and non-first-episode SZ patients who received antipsychotics before enrollment. The Prodromal Questionnaire was used to confirm the absence of any psychotic syndromes in HCs (Loewy et al., 2005). Exclusion criteria for the patient groups were also applied to HCs who were assessed by two senior clinical psychiatrists.

Table 1
Demographic and clinical characteristics of patients with AVHs (n =25), patients without AVHs (n =25), and HCs (n =25).

Characteristics	AVHs patients	Non-AVHs patients	HCs
Age (years)	24 ± 7	24 ± 5	26 ± 5
Sex (male/female)	14/11	13/12	12/13
Education (years)	14 ± 2	14 ± 2	15 ± 2
Handness (right/left)	25/0	25/0	25/0
Duration of illness (months)	14 ± 19	18 ± 21	—
First episode (yes/no)	17/8	21/4	—
PANSS Total Score	109 ± 12*	92 ± 22	—
PANSS Positive Score	31 ± 6*	21 ± 9	—
PANSS Negative Score	27 ± 4	23 ± 10	—
PANSS General Psychopathology	52 ± 8	48 ± 9	—
AHRS Score	27 ± 5	—	—

Data are mean ± SD. *P < 0.05 versus Non-AVHs patients. PANSS, Positive and Negative Syndrome Scale; AHRS, Auditory Hallucination Rating Scale.

2.2. Image acquisition

Imaging was performed on a Siemens 3.0T Trio MR scanner (Erlangen, Germany) using the body coil for transmission and an eight channel head coil for reception. A 10-min 3D magnetization-prepared, rapid acquisition gradient echo (MPRAGE: 192 slices, voxel size =1 mm×1 mm×1 mm, matrix =256×256, slice thickness =1 mm, gap =0 mm, field of view =256 mm×256 mm, repetition time =2530 ms, echo time =3.5 ms) image was first acquired to obtain a high-resolution T1-weighted anatomical image for spatial normalization and overlays of functional data. The resting state perfusion imaging was performed using a pulsed ASL (pASL) sequence (repetition time =2805 ms, echo time =13 ms, post-label delay =1800 ms, flip angle =90°; voxel size =4 mm×4 mm×3 mm; field of view =256 mm×256 mm; reconstruction matrix =256×256; slice thickness =3 mm, gap =0.75 mm; 31 axial slices). The total acquisition time for the resting state ASL scan was 4 min and 20 s. Earplugs and a custom-built head cushion were used to dampen scanner noise and minimize head motion, reducing motion artifacts during acquisition to avoid poor imaging quality. During the ASL scans, all subjects were instructed to keep their eyes closed, relax without movement, think of nothing in particular, and not fall asleep. They were judged to be awake at the beginning and end of the scanning, and they were sure to have been keeping awake. Image quality was controlled automatically using the PICORE perfusion mode and we had a careful check on images of each subject before further analysis, thereby ensuring the quality of data.

2.3. CBF calculation

Data analysis was carried out in Arterial Spin Labeling Perfusion MRI Signal Processing Toolbox (ASLtbx; http://cfn.upenn.edu/~wangze/ASLtbx.php) according to Wang et al. (Hu et al., 2010; Wang, 2012; Wang et al., 2008). The detailed procedures have been described in these previous studies, partly based on SPM12 (http://www.fil.ion.ucl.ac.uk/spm/), including image reorientation, motion correction, coregistering to each participant's structural scan then to positron emission tomography (PET)-perfusion templates and final to Montreal Neurological Institute (MNI) space using affine transformation, spatial smoothing with a Gaussian kernel of 6 mm full-width at half-maximum (FWHM), removing non-brain tissue, and CBF quantification. Additionally, as Zhu et al. implemented (Zhu et al., 2016), we have calculated the Jenkinson's mean frame-wise displacement as a measure of the micro-head motion of each subject.

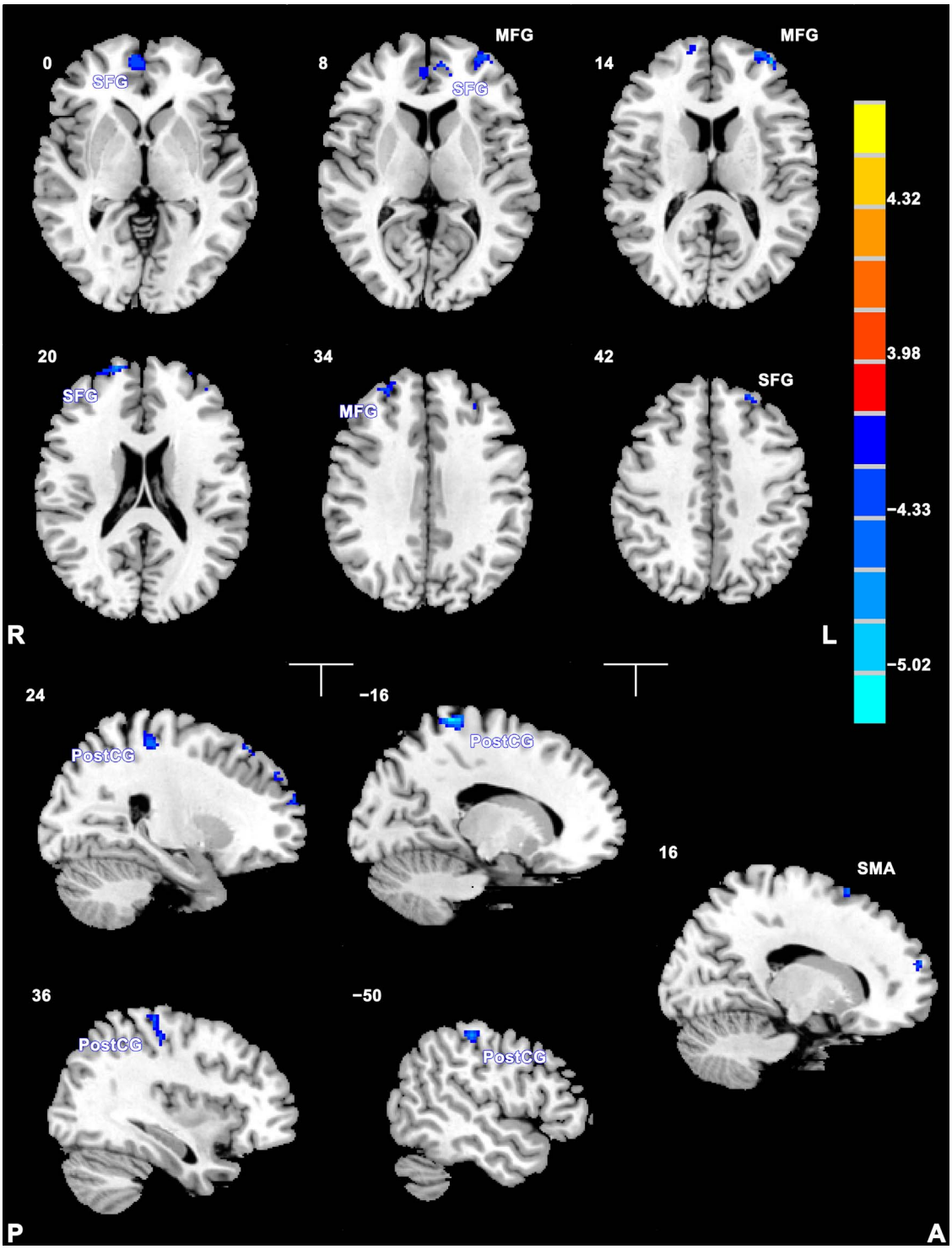

Fig. 1. Brain regions with significant CBF differences between SZ patients with and without AVHs. The warm color represents increased CBF, and the cold color denotes decreased CBF. MFG, middle frontal gyrus; PostCG, postcentral gyrus; SFG, superior frontal gyrus; SMA, supplementary motor area.

2.4. Statistical analysis

The group differences in CBF were compared in a voxel-wise manner using a two-sample *t*-test. There was no significant difference in demographic data (Table 1) and mean frame-wise displacement (AVHs: 0.16 ± 0.14 mm; Non-AVHs: 0.14 ± 0.07 mm; HCs: 0.12 ± 0.06 mm; P=0.38) among these groups. When performing statistical analysis, we did not apply age, sex, education, duration of illness, and mean frame-wise displacement as covariates for regression. Multiple comparisons were corrected using the AlphaSim method ($P < 0.001$, cluster extent ≥13 for cluster $P < 0.05$) on the basis of the Correction Thresholds by AlphaSim module of Resting-State fMRI Data Analysis Toolkit V1.8 (http://www.restfmri.net/forum/REST_V1.8). For each subject, the average CBF value of each cluster with a significant group difference was extracted and used for correlation and receiver operating characteristic (ROC) analyses. Pearson correlation coefficients between brain function measures (CBF value) and the severity of symptoms (AHRS and PANSS scores) were separately computed for each patient group. In addition, ROC analysis was used to assess the diagnostic capability of these imaging measures to

distinguish SZ patients with AVHs from those without AVHs. ROC curves are being used to judge the discrimination ability of test results (Hanley and McNeil, 1982), and a larger area under ROC curve indicates a higher accuracy of diagnostic performance. Correlation and ROC analyses were performed with SPSS software (version 13.0, SPSS, Inc.). Significance was set at $P < 0.05$ with Bonferroni correction for multiple comparisons in the correlation analysis.

2.5. CBF connectivity analysis

A full description of this CBF connectivity approach is available as reported by Melie-Garcia et al. (Melie-Garcia et al., 2013). First, using the automated anatomical labeling (AAL) atlas (Tzourio-Mazoyer et al., 2002) that parcillates the whole brain (without the cerebellum) into 90 regions, brain parcellation was conducted to the preceding preprocessed CBF images for all the subjects in the same group (SZ patients with AVHs, SZ patients without AVHs, and HCs), yielding three matrices with "n" (number of subjects) rows by 90 columns. Each column represents the average CBF value of each region, respectively. Second, we defined a connection as the Pearson correlation of CBF value between each column, which generates a 90 by 90 CBF connectivity matrix for each group. Fisher's z test was used for comparing correlations between two independent groups (http://www.fon.hum.uva.nl/Service/Statistics/Two_Correlations.html). Finally, we calculated network properties to characterize brain CBF network. These CBF network properties (characteristics path length, clustering index, local efficiency, and global efficiency) were calculated over a range of sparsity values from 0.5 to 0.9, by step 0.05. Characteristics path length and global efficiency are the commonly used for measuring functional integration. The average shortest path length between all pairs of nodes in the network is known as the characteristic path length of the network, and the average inverse shortest path length is a related measure known as the global efficiency (Rubinov and Sporns, 2010). Measures of functional segregation comprise clustering index and local efficiency. The fraction of triangles around an individual node is known as the clustering index and is equivalent to the fraction of the node's neighbors that are also neighbors of each other (Watts and Strogatz, 1998). The local efficiency reflects the fault tolerance of the network, which indicates how well the information is communicated within the neighbors of a given node when this node is eliminated (Latora and Marchiori, 2001).

3. Results

3.1. Group differences of CBF

The CBF differences between SZ patients with and without AVHs are shown in Fig. 1 and Table 2. AVHs patients exhibited decreased CBF in the bilateral superior and middle frontal gyri and postcentral gyri, and right supplementary motor area compared with SZ patients without AVHs. In contrast to HCs, AVHs displayed attenuated CBF in the bilateral superior and middle frontal gyri and precentral gyri, as well as the left inferior parietal lobule, inferior frontal gyrus, insula, and the right postcentral gyrus, angular gyrus and caudate. Moreover, SZ patients without AVHs showed reduced CBF in the left middle frontal gyrus relative to HCs.

3.2. Correlations between CBF and clinical data, and ROC analyses

CBF values in regions with significant differences were not correlated with AHRS and PANSS positive factor scores (Table S1). ROC analyses revealed the capacity of CBF values in discriminating SZ patients with AVHs from those without AVHs. In addition, areas under ROC curves of reduced and increased CBF are listed in Table 3.

Table 2
Brain regions with significant differences in CBF.

Regions	Cluster size	Peak t value	x	y	z
AVHs < Non-AVHs					
Right superior frontal gyrus	73	−4.6526	18	62	20
Right superior frontal gyrus	25	−4.4305	24	30	54
Right medial superior frontal gyrus	130	−4.289	6	56	0
Left medial superior frontal gyrus	16	−4.2936	−10	52	8
Left superior frontal gyrus	14	−4.2184	−26	42	42
Right middle frontal gyrus	22	−4.3143	26	48	34
Left middle frontal gyrus	127	−4.8361	−38	54	14
Left middle frontal gyrus	19	−4.1254	−32	38	36
Right postcentral gyrus	63	−4.4324	24	−34	58
Right postcentral gyrus	48	−4.3835	36	−30	62
Left postcentral gyrus	50	−4.6303	−50	−28	52
Left postcentral gyrus	112	−5.2454	−16	−40	72
Right supplementary motor area	13	−4.5152	16	16	66
Non-AVHs < HCs					
Left middle frontal gyrus	16	−4.2904	−42	54	22

$P < 0.001$ (correction thresholds by AlphaSim).

Table 3
Area under ROC curve.

Regions	Area	95% CI
AVHs < Non-AVHs		
Right superior frontal gyrus	0.87	0.77, 0.97
Right superior frontal gyrus	0.81	0.69, 0.93
Right medial superior frontal gyrus	0.87	0.77, 0.97
Left medial superior frontal gyrus	0.84	0.73, 0.95
Left superior frontal gyrus	0.81	0.70, 0.93
Right middle frontal gyrus	0.84	0.74, 0.95
Left middle frontal gyrus	0.88	0.78, 0.97
Left middle frontal gyrus	0.80	0.68, 0.92
Right postcentral gyrus	0.83	0.72, 0.95
Right postcentral gyrus	0.83	0.71, 0.94
Left postcentral gyrus	0.84	0.73, 0.95
Left postcentral gyrus	0.84	0.73, 0.95
Right supplementary motor area	0.82	0.70, 0.94

CI, confidence interval.

3.3. Patterns of CBF connectivity

In the present study, we estimated the matrices of CBF concurrent changes between 90 brain anatomical structures defined in the AAL atlas in three groups (Fig. 2). The rows of brain areas with significant group differences in the CBF were marked when presenting connectivity matrix in three groups. Fig. 3 presents connections with correlation coefficient value larger than 0.6 or less than −0.6 (representing P level of the correlation coefficient at 0.05 with false discovery rate correction). Using the method by Melie-Garcia et al., we could only calculate one matrix for each group (Melie-Garcia et al., 2013), leading to the incapability for comparing the difference between groups. We then used Fisher's z test to compare correlations between two groups. Table 4 shows the z values of significantly different connectivity between AVHs and Non-AVHs patients.

Notably, SZ patients with AVHs revealed relatively long characteristic path length, small clustering index, and low local efficiency (Fig. 4A–C), as well as relatively high global efficiency (Fig. 4D) in contrast to patients without AVHs. Generally, both SZ patient groups showed measurements of decreased connectivity within the network compared with HCs.

4. Discussion

In the current study, we detected lower level of CBF in the bilateral

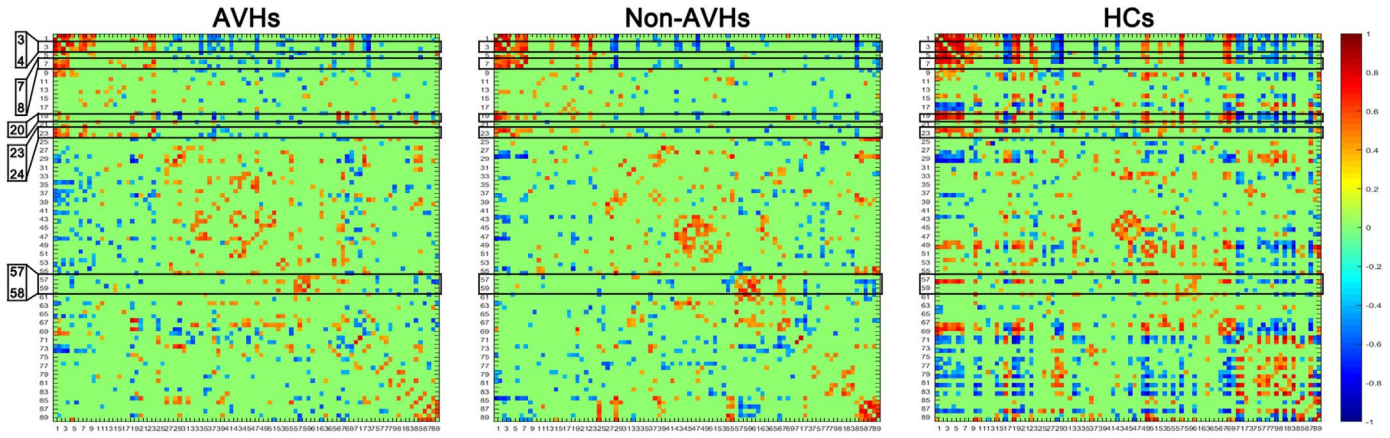

Fig. 2. The CBF connectivity matrix obtained by calculating Pearson's correlation between regional CBF across subjects. Numbers in AAL atlas on the left side refer to different brain regions with significant CBF differences between SZ patients with and without AVHs. 3, Frontal_Sup_L, left superior frontal gyrus; 4, Frontal_Sup_R, right superior frontal gyrus; 7, Frontal_Mid_L, left middle frontal gyrus; 8, Frontal_Mid_R, right middle frontal gyrus; 20, Supp_Motor_Area_R, right supplementary motor area; 23, Frontal_Sup_Medial_L, left medial superior fontal gyrus; 24, Frontal_Sup_Medial_R, right medial superior fontal gyrus; 57, Postcentral_L, left postcentral gyrus; 58, Postcentral_R, right postcentral gyrus. The color bar indicates the correlation coefficient value.(For interpretation of the references to color in this figure legend, the reader is referred to the web version of this article).

dorsolateral prefrontal cortices (DLPFC) of SZ patients with AVHs relative to those without AVHs, in line with one of the most influential cognitive models that proposes the impairment of self-monitoring on one's own inner speech, then misleading to identify verbal thoughts as alien source (Moseley et al., 2013). Then we also found decrease of CBF in the left supplementary motor area and bilateral postcentral gyri, which involve speech imagery (supplementary motor area) (McGuire et al., 1995; Raij and Riekki, 2012) and production (postcentral gyrus) (Tremblay et al., 2003). Moreover, this CBF measure might be an effective indicator of AVHs vulnerability in SZ on the basis of ROC analysis. The complex network analysis demonstrated dysfunctional CBF connectivity of SZ patients with AVHs. Our findings extend the current thinking about AVHs by: (1) linking the speech imagery region (supplementary motor area) with AVHs in SZ, and (2) detecting CBF connectivity pattern in AVHs, an intermediate network level between HCs and Non-AVHs.

Several previous studies have applied ASL to investigate resting state CBF characteristics in SZ patients (Kindler et al., 2015; Pinkham et al., 2011; Scheef et al., 2010; Zhu et al., 2015) and CBF alteration in SZ patients with AVHs receiving TMS (Homan et al., 2013). In our study, both patient groups revealed lower level of CBF in the left frontal middle gyrus, which has been detected in SZ patients by Zhu et al., Scheef et al. and Kinder et al. (Kindler et al., 2015; Scheef et al., 2010; Zhu et al., 2015). With the exception of the left middle frontal gyrus, Zhu et al. found decreased CBF in the left insula (Zhu et al., 2015), which is also our findings in SZ patients suffering from AVHs compared with HCs. Besides, there are a few contradictory findings among these studies. Symptoms-based subtyping (i.e., AVHs and Non-AVHs) and subjects' clinical heterogeneity in our present study might lead to this discrepancy. Another possible factor is the sequence used, i.e., pASL in our study and pseudocontinuous ASL (pcASL) in theirs. According to the consensus in a "ASL white paper", the signal-to-noise ratio (SNR) of the pcASL approach is higher than that of pASL, but pASL uses a single short pulse or a limited number of pulses to invert a thick slab of arterial water spins, which is superior at high magnetic strength field (Alsop et al., 2015). Additionally, Zhu et al. and Liu et al. performed across-subject CBF connectivity analysis using a larger sample size of SZ patients (Liu et al., 2016; Zhu et al., 2015), but they did not divide patients into groups based on symptoms.

Back to our findings, firstly, we found extensive CBF reduction in the bilateral DLPFC in SZ patients with AVHs. PFC is connected directly with almost every distinct cerebral functional unit (Nauta, 1972). These unique connections make it singularly suited for coordinating and integrating the function of other brain regions (Hofer and Frahm, 2006). DLPFC constitutes a major part of PFC and appears to function as monitoring speech production in language processing, particularly in AVHs sufferers of SZ patients (Mondino et al., 2016). An increasing number of fMRI studies of SZ patients have shown atypical function of DLPFC to be related to AVHs (Clos et al., 2014; Hoffman et al., 2011; Kawaguchi et al., 2005; Lawrie et al., 2002; Sommer et al., 2012). Previous studies have demonstrated the linkage between DLPFC and AVHs in SZ.

With functional connectivity analysis, Lawrie et al. found hypoconnectivity between the left DLPFC and middle/superior temporal gyrus was negatively correlated with the severity of AVHs in SZ during language tasks (Lawrie et al., 2002). At resting state, the left DLPFC revealed significantly greater coupling with Wernicke's area in SZ patients with AVHs when compared with those without AVHs (Hoffman et al., 2011). Furthermore, Sommer et al. found hypoconnectivity between the left DLPFC and inferior frontal gyrus (representing Broca's area) (Clos et al., 2014; Sommer et al., 2012). Using a spatially filtered magnetoencephalography analysis, Kawaguchi et al. also demonstrated dysfunction in the left DLPFC in relation to AVHs in SZ (Kawaguchi et al., 2005). In line with these previous findings without external intervention, DLPFC is also regulated by tDCS or TMS mentioned below for AVHs in SZ.

Clinically, refractory AVHs in SZ were robustly reduced by tDCS (Andrade, 2013; Brunelin et al., 2012; Mondino et al., 2016) using the most employed montage with the anode placed over the left DLPFC and the cathode over the left temporo-parietal junction (TPJ) (Brunoni et al., 2014). Another tool is repetitive TMS (rTMS) for treatment of AVHs in SZ. For one thing, by means of functional connectivity analysis, not only tDCS but also rTMS increase the coupling between the left TPJ and DLPFC (Gromann et al., 2012; Mondino et al., 2016). For another, rTMS enhances regional activation of the left DLPFC in SZ patients suffering from AVHs (Lennox et al., 2000), providing evidence for the possible mechanism that underlies therapeutic effect of these methods on AVHs in SZ. It has been postulated that the predisposition to suffer from AVHs in SZ results from decoupling between speech producing and self-monitoring, involving supplementary motor area and DLPFC, respectively (Clos et al., 2014). Our results demonstrate reduced activation of the self-monitoring system (DLPFC) for inner speech in terms of CBF in SZ patients with AVHs.

Next, as compared with SZ patients without AVHs, these AVHs patients showed decreased CBF in the right supplementary motor area in our present study. In spite of no typical report about the activation of supplementary motor area in functional imaging studies that have compared AVHs-related brain activation (Allen et al., 2012; Jardri

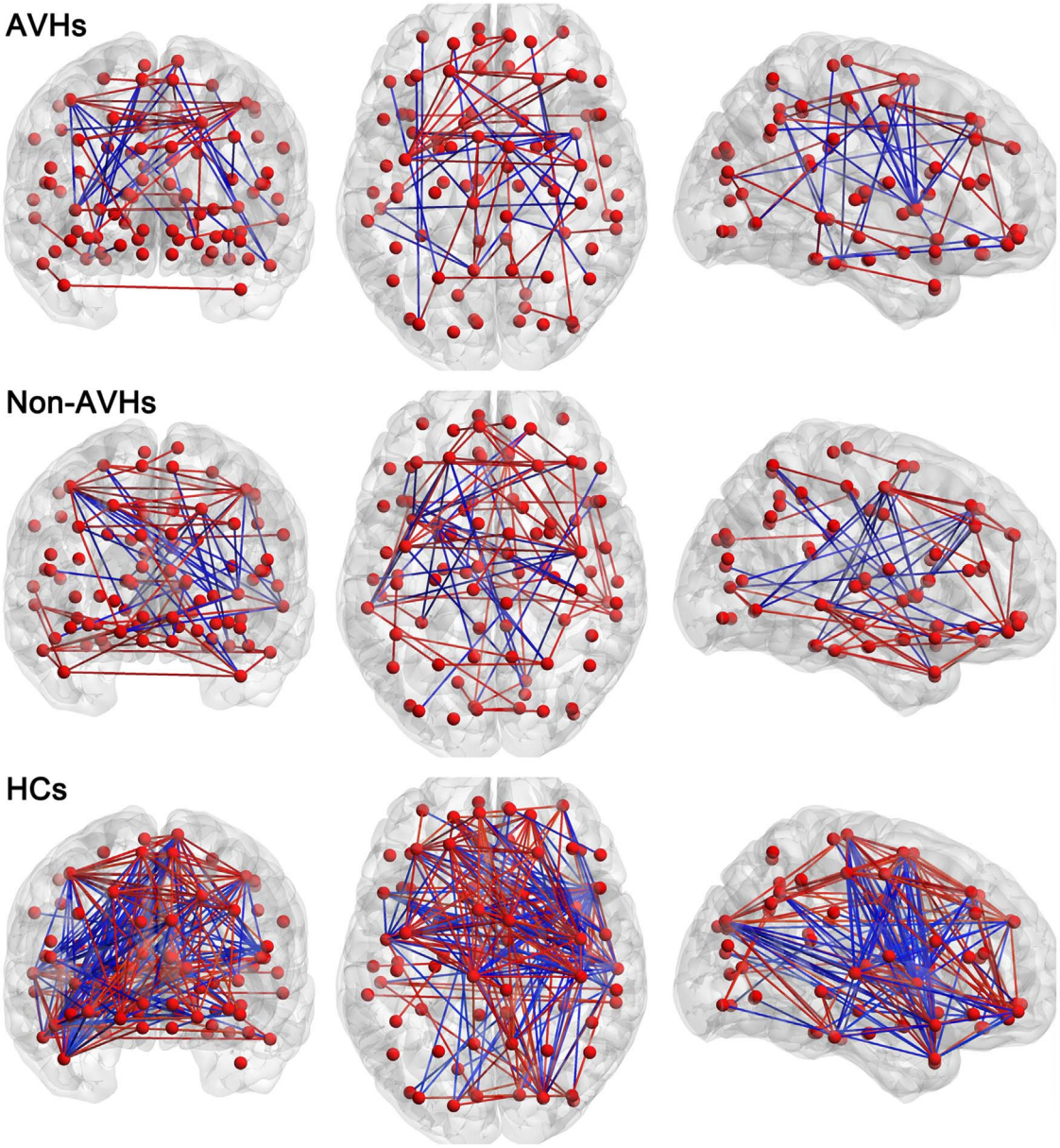

Fig. 3. The CBF networks showing connections with correlation coefficient value larger than 0.6 or less than −0.6. Line color indicates the positive (red) or negative (blue) coefficient. (For interpretation of the references to color in this figure legend, the reader is referred to the web version of this article).

et al., 2011), in a seminal study by McGuire et al. (McGuire et al., 1995), the supplementary motor area activated more weakly during verbal imagery in SZ patients with AVHs than in HCs. Furthermore, Raij et al. found that the activation of supplementary motor area was weaker during AVHs than during verbal imagery in SZ patients with AVHs (Raij and Riekki, 2012). Therefore, our results involving CBF of the supplementary motor area strongly suggest its functional deficit might relate to "the loss of the sense that the inner speech is self-generated", as interpreted by McGuire et al. (McGuire et al., 1995).

Finally, in our previous voxel-mirrored homotopic connectivity study, SZ patients with AVHs have decreased inter-hemispheric connectivity between the bilateral superior parietal gyrus and anterior cingulate cortices, and negative correlations of the connectivity with PANSS positive score (Chang et al., 2015). In the present study, CBF levels symmetrically reduced in the bilateral postcentral gyri. In other words, we detected the altered function in the bilateral homotopic regions of the brain, which were revealed by different sequences and data analysis approaches. What's more, volumetric MRI studies implicate specific relationships between the volume reduction of bilateral postcentral gyri and severity of AVHs in SZ (Garcia-Marti et al., 2008; Nenadic et al., 2010). Our results further provide the evidence of AVHs in SZ sufferers with the discrepant function in the bilateral postcentral gyri in addition to anomalous structure. A meta-analysis by Kühn et al. (Kuhn and Gallinat, 2012), included studies comparing periods of presence and absence of AVHs, has established the association of AVHs in SZ with activation in the bilateral postcentral gyri, brain regions related to subvocal speech (Stephane et al., 2001), and therefore being considered involving inner speech production.

Using the methodology mentioned above, we performed CBF

Table 4
z values of significantly different connectivity with regions of different CBF between AVHs and Non-AVHs patients.

Connectivity	*z* values	*P* values
Left SFG-left orbital SFG	2.9376	0.0107
Left SFG- left medial SFG	−3.2870	0.0036
Left SFG- left fusiform gyrus	2.8833	0.0125
Left SFG-right putamen	−3.0013	0.0088
Left SFG-left MTG	2.8012	0.0158
Right SFG-right putamen	−3.4944	0.0018
Left MFG-right MFG	−3.6714	0.0009
Left MFG-left insula	2.8746	0.0128
Right MFG-left insula	3.5115	0.0017
Right SMA-left PreCG	−3.6088	0.0012
Right SMA-right hippocampus	−3.0035	0.0088
Right SMA-left pallidum	3.2249	0.0044
Left medial SFG-right medial SFG	2.8878	0.0123
Left PostCG-left angular gyrus	−2.8430	0.0140
Right PostCG-right IOG	3.7866	0.0006

IOG, inferior occipital gyrus; MFG, middle frontal gyrus; MTG, middle temporal gyrus; PreCG, precentral gyrus; PostCG, postcentral gyrus; SFG, superior frontal gyrus; SMA, supplementary motor area; SPG, superior parietal gyrus.

connectivity and analyzed characteristics of its network. In contrast to functional connectivity using BOLD data, influenced by multiple physiological parameters, CBF connectivity is more definitely physiologically implicated and modulated by regional CBF merely. The computed global network properties, including clustering index, characteristic path length, local efficiency, and global efficiency, suggest SZ patients are not able to so efficiently transfer information within functional brain network, and they have weakened capacity against disturbance relative to HCs (Rubinov and Sporns, 2010). Likewise, SZ patients with AVHs possessed three network characteristics with values next to patients without AVHs. Importantly, they also had one property, global efficiency, with an intermediate level between HCs and patients who did not experience AVHs, implying an active integration in larger and sparser network (Estrada and Hatano, 2008). Our study provides a comprehensive description of the network arisen from CBF concurrent fluctuations among brain areas for AVHs in SZ.

We need to acknowledge several limitations of the current study. First, there was no significant correlation between CBF values and AHRS/PANSS positive factor scores, merely implicating the brain dysfunction in relation to the trait – but not the severity – of AVHs. To examine subtle differences among subtypes in SZ, i.e., AVHs in our study, unsupervised machine learning methods may be a better selection, since unsupervised machine learning approaches can discover homogeneous groups of similar samples within the data and flexibly determine the complex and unknown distribution or pattern of data within the input space without prior knowledge (Zeng et al., 2014a). We are with the belief of that unsupervised clustering analysis is a potential future direction for the subtypes in SZ. Second, the information of treatment (e.g., drugs, dose, and period of treatment) was inadequate in the current study so that we were unable to evaluate the effect of antipsychotics on patients' cerebral function. Still, we

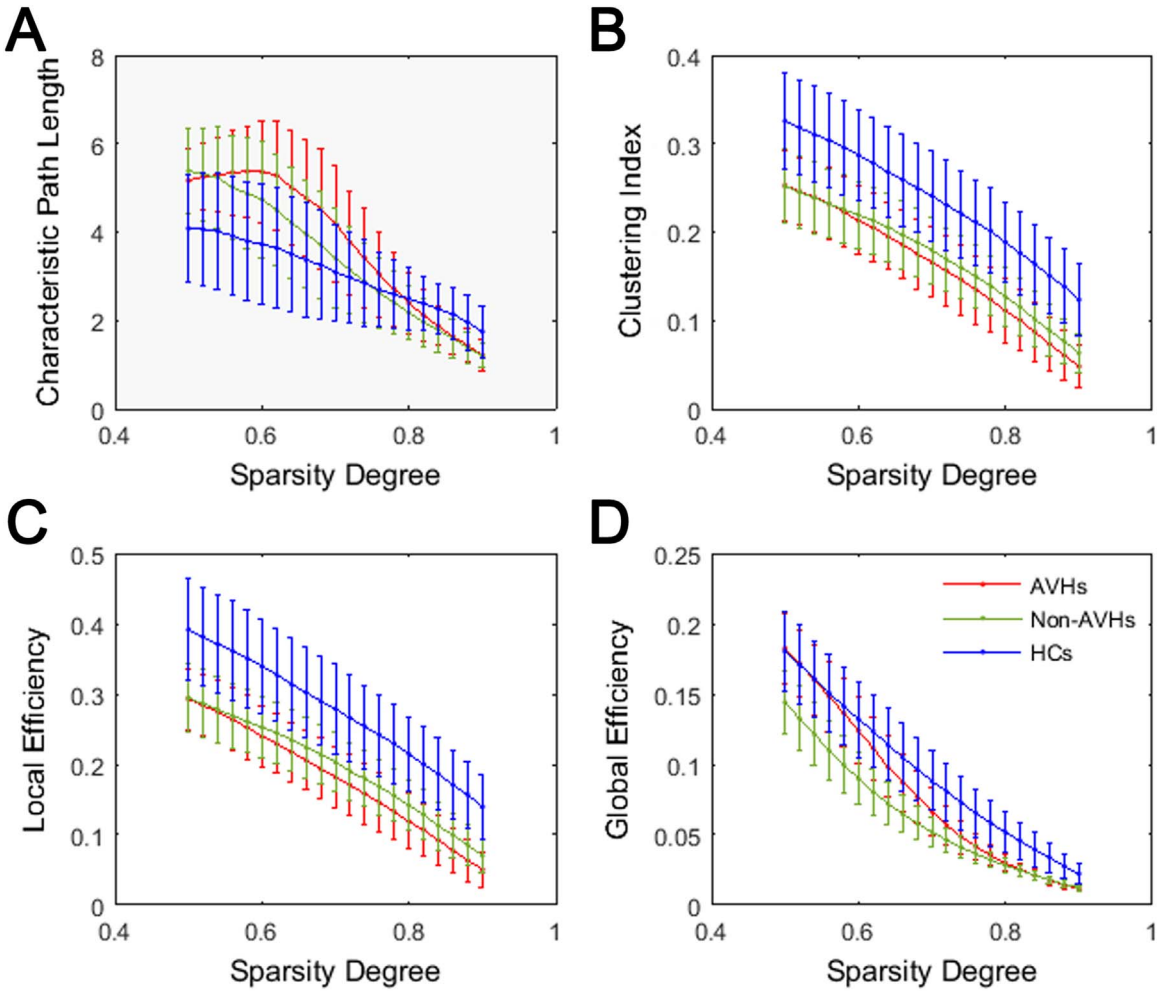

Fig. 4. Global network properties as function of sparsity degree. The characteristic path length, clustering index, local efficiency, and global efficiency decrease as the sparsity degree increases.

suggest that the pursuit for neural mechanisms underlying AVHs in SZ is important but that it requires substantial additional effort and investment before we can reap the rewards of both preclinical and clinical benefits.

In conclusion, the current study demonstrates aberrant CBF in the brain regions including bilateral DLPFC (inner speech monitoring) and postcentral gyri (speech production), as well as right supplementary motor area (speech imagery) in SZ patients with AVHs compared with those without AVHs. Furthermore, the complex network measures showed by the CBF network indicates distinct pattern in the communication between different functional units within the network of AVHs in SZ.

Contributors

HY and Y-BX guaranteed the integrity of entire study and designed the study. All authors contributed to data acquisition or data analysis/interpretation, manuscript drafting or manuscript revision for important intellectual content, and approval of final version of submitted manuscript. L-BC, GC, Z-LX, and LL performed statistical analysis. L-BC, GC, and Z-LX conducted the literature research.

Conflicts of interest

The authors have no conflict of interest to declare. This work was supported by National Natural Science Foundation of China (No. 81571651), National Key Basic Research and Development Program (973) (No. 2011CB707805), and Fund for the Dissertation Submitted to Fourth Military Medical University for the Academic Degree of Doctor (No. 2014D07). The funding source had no role in the design and conduct of the study, analysis or interpretation of the data, preparation or final approval of the manuscript, or the decision to submit the manuscript for publication.

Acknowledgements

Prof Ze Wang at Perelman School of Medicine, University of Pennsylvania and Dr Yuanqiang Zhu at School of Life Sciences and Technology, Xidian University provided helpful comments on data processing and manuscript revision, respectively, for which we are very grateful.

Appendix A. Supporting information

Supplementary data associated with this article can be found in the online version at doi:10.1016/j.pscychresns.2016.12.006.

References

Allen, P., Modinos, G., Hubl, D., Shields, G., Cachia, A., Jardri, R., Thomas, P., Woodward, T., Shotbolt, P., Plaze, M., Hoffman, R., 2012. Neuroimaging auditory hallucinations in schizophrenia: from neuroanatomy to neurochemistry and beyond. Schizophr. Bull. 38, 695–703.

Alsop, D.C., Detre, J.A., Golay, X., Gunther, M., Hendrikse, J., Hernandez-Garcia, L., Lu, H., MacIntosh, B.J., Parkes, L.M., Smits, M., van Osch, M.J., Wang, D.J., Wong, E.C., Zaharchuk, G., 2015. Recommended implementation of arterial spin-labeled perfusion MRI for clinical applications: a consensus of the ISMRM perfusion study group and the European consortium for ASL in dementia. Magn. Reson. Med. 73, 102–116.

Andrade, C., 2013. Transcranial direct current stimulation for refractory auditory hallucinations in schizophrenia. J. Clin. Psychiatry 74, e1054–e1058.

APA, 2013. Diagnostic and Statistical Manual of Mental Disorders 5th ed. American Psychiatric Association, Washington, DC, 87–118.

Brunelin, J., Mondino, M., Gassab, L., Haesebaert, F., Gaha, L., Suaud-Chagny, M.F., Saoud, M., Mechri, A., Poulet, E., 2012. Examining transcranial direct-current stimulation (tDCS) as a treatment for hallucinations in schizophrenia. Am. J. Psychiatry 169, 719–724.

Brunoni, A.R., Shiozawa, P., Truong, D., Javitt, D.C., Elkis, H., Fregni, F., Bikson, M., 2014. Understanding tDCS effects in schizophrenia: a systematic review of clinical data and an integrated computation modeling analysis. Expert Rev. Med Dev. 11, 383–394.

Chang, X., Xi, Y.B., Cui, L.B., Wang, H.N., Sun, J.B., Zhu, Y.Q., Huang, P., Collin, G., Liu, K., Xi, M., Qi, S., Tan, Q.R., Miao, D.M., Yin, H., 2015. Distinct inter-hemispheric dysconnectivity in schizophrenia patients with and without auditory verbal hallucinations. Sci. Rep. 5, 11218.

Clos, M., Diederen, K.M., Meijering, A.L., Sommer, I.E., Eickhoff, S.B., 2014. Aberrant connectivity of areas for decoding degraded speech in patients with auditory verbal hallucinations. Brain Struct. Funct. 219, 581–594.

Cui, L.B., Liu, K., Li, C., Wang, L.X., Guo, F., Tian, P., Wu, Y.J., Guo, L., Liu, W.M., Xi, Y.B., Wang, H.N., Yin, H., 2016. Putamen-related regional and network functional deficits in first-episode schizophrenia with auditory verbal hallucinations. Schizophr. Res 173, 13–22.

Du, A.T., Jahng, G.H., Hayasaka, S., Kramer, J.H., Rosen, H.J., Gorno-Tempini, M.L., Rankin, K.P., Miller, B.L., Weiner, M.W., Schuff, N., 2006. Hypoperfusion in frontotemporal dementia and Alzheimer disease by arterial spin labeling MRI. Neurology 67, 1215–1220.

Estrada, E., Hatano, N., 2008. Communicability in complex networks. Phys. Rev. E Stat. Nonlin Soft Matter Phys. 77, 036111.

Garcia-Marti, G., Aguilar, E.J., Lull, J.J., Marti-Bonmati, L., Escarti, M.J., Manjon, J.V., Moratal, D., Robles, M., Sanjuan, J., 2008. Schizophrenia with auditory hallucinations: a voxel-based morphometry study. Prog. Neuropsychopharmacol. Biol. Psychiatry 32, 72–80.

Gromann, P.M., Tracy, D.K., Giampietro, V., Brammer, M.J., Krabbendam, L., Shergill, S.S., 2012. Examining frontotemporal connectivity and rTMS in healthy controls: implications for auditory hallucinations in schizophrenia. Neuropsychology 26, 127–132.

Hanley, J.A., McNeil, B.J., 1982. The meaning and use of the area under a receiver operating characteristic (ROC) curve. Radiology 143, 29–36.

Hofer, S., Frahm, J., 2006. Topography of the human corpus callosum revisited–Comprehensive fiber tractography using diffusion tensor magnetic resonance imaging. Neuroimage 32, 989–994.

Hoffman, R.E., Fernandez, T., Pittman, B., Hampson, M., 2011. Elevated functional connectivity along a corticostriatal loop and the mechanism of auditory/verbal hallucinations in patients with schizophrenia. Biol. Psychiatry 69, 407–414.

Hoffman, R.E., Hawkins, K.A., Gueorguieva, R., Boutros, N.N., Rachid, F., Carroll, K., Krystal, J.H., 2003. Transcranial magnetic stimulation of left temporoparietal cortex and medication-resistant auditory hallucinations. Arch. Gen. Psychiatry 60, 49–56.

Homan, P., Kindler, J., Federspiel, A., Flury, R., Hubl, D., Hauf, M., Dierks, T., 2011. Muting the voice: a case of arterial spin labeling-monitored transcranial direct current stimulation treatment of auditory verbal hallucinations. Am. J. Psychiatry 168, 853–854.

Homan, P., Kindler, J., Hauf, M., Walther, S., Hubl, D., Dierks, T., 2013. Repeated measurements of cerebral blood flow in the left superior temporal gyrus reveal tonic hyperactivity in patients with auditory verbal hallucinations: a possible trait marker. Front Hum. Neurosci. 7, 304.

Hu, W.T., Wang, Z., Lee, V.M., Trojanowski, J.Q., Detre, J.A., Grossman, M., 2010. Distinct cerebral perfusion patterns in FTLD and AD. Neurology 75, 881–888.

Huang, P., Xi, Y., Lu, Z.L., Chen, Y., Li, X., Li, W., Zhu, X., Cui, L.B., Tan, Q., Liu, W., Li, C., Miao, D., Yin, H., 2015. Decreased bilateral thalamic gray matter volume in first-episode schizophrenia with prominent hallucinatory symptoms: a volumetric MRI study. Sci. Rep. 5, 14505.

Jardri, R., Pouchet, A., Pins, D., Thomas, P., 2011. Cortical activations during auditory verbal hallucinations in schizophrenia: a coordinate-based meta-analysis. Am. J. Psychiatry 168, 73–81.

Kawaguchi, S., Ukai, S., Shinosaki, K., Ishii, R., Yamamoto, M., Ogawa, A., Mizuno-Matsumoto, Y., Fujita, N., Yoshimine, T., Takeda, M., 2005. Information processing flow and neural activations in the dorsolateral prefrontal cortex in the Stroop task in schizophrenic patients. A spatially filtered MEG analysis with high temporal and spatial resolution. Neuropsychobiology 51, 191–203.

Kay, S.R., Fiszbein, A., Opler, L.A., 1987. The positive and negative syndrome scale (PANSS) for schizophrenia. Schizophr. Bull. 13, 261–276.

Kindler, J., Homan, P., Jann, K., Federspiel, A., Flury, R., Hauf, M., Strik, W., Dierks, T., Hubl, D., 2013. Reduced neuronal activity in language-related regions after transcranial magnetic stimulation therapy for auditory verbal hallucinations. Biol. Psychiatry 73, 518–524.

Kindler, J., Jann, K., Homan, P., Hauf, M., Walther, S., Strik, W., Dierks, T., Hubl, D., 2015. Static and dynamic characteristics of cerebral blood flow during the resting state in schizophrenia. Schizophr. Bull. 41, 163–170.

Kuhn, S., Gallinat, J., 2012. Quantitative meta-analysis on state and trait aspects of auditory verbal hallucinations in schizophrenia. Schizophr. Bull. 38, 779–786.

Latora, V., Marchiori, M., 2001. Efficient behavior of small-world networks. Phys. Rev. Lett. 87, 198701.

Lawrie, S.M., Buechel, C., Whalley, H.C., Frith, C.D., Friston, K.J., Johnstone, E.C., 2002. Reduced frontotemporal functional connectivity in schizophrenia associated with auditory hallucinations. Biol. Psychiatry 51, 1008–1011.

Lennox, B.R., Park, S.B., Medley, I., Morris, P.G., Jones, P.B., 2000. The functional anatomy of auditory hallucinations in schizophrenia. Psychiatry Res. 100, 13–20.

Liu, F., Zhuo, C., Yu, C., 2016. Altered cerebral blood flow covariance network in schizophrenia. Front Neurosci. 10, 308.

Loewy, R.L., Bearden, C.E., Johnson, J.K., Raine, A., Cannon, T.D., 2005. The prodromal questionnaire (PQ): preliminary validation of a self-report screening measure for prodromal and psychotic syndromes. Schizophr. Res. 79, 117–125.

Logothetis, N.K., Pauls, J., Augath, M., Trinath, T., Oeltermann, A., 2001. Neurophysiological investigation of the basis of the fMRI signal. Nature 412, 150–157.

McGuire, P.K., Silbersweig, D.A., Wright, I., Murray, R.M., David, A.S., Frackowiak, R.S., Frith, C.D., 1995. Abnormal monitoring of inner speech: a physiological basis for

auditory hallucinations. Lancet 346, 596–600.
Melie-Garcia, L., Sanabria-Diaz, G., Sanchez-Catasus, C., 2013. Studying the topological organization of the cerebral blood flow fluctuations in resting state. Neuroimage 64, 173–184.
Mondino, M., Jardri, R., Suaud-Chagny, M.F., Saoud, M., Poulet, E., Brunelin, J., 2016. Effects of fronto-temporal transcranial direct current stimulation on auditory verbal hallucinations and resting-state functional connectivity of the left temporo-parietal junction in patients with schizophrenia. Schizophr. Bull. 42, 318–326.
Moseley, P., Fernyhough, C., Ellison, A., 2013. Auditory verbal hallucinations as atypical inner speech monitoring, and the potential of neurostimulation as a treatment option. Neurosci. Biobehav Rev. 37, 2794–2805.
Nauta, W.J., 1972. Neural associations of the frontal cortex. Acta Neurobiol. Exp. (Wars.) 32, 125–140.
Nenadic, I., Smesny, S., Schlosser, R.G., Sauer, H., Gaser, C., 2010. Auditory hallucinations and brain structure in schizophrenia: voxel-based morphometric study. Br. J. Psychiatry 196, 412–413.
Pinkham, A., Loughead, J., Ruparel, K., Wu, W.C., Overton, E., Gur, R., 2011. Resting quantitative cerebral blood flow in schizophrenia measured by pulsed arterial spin labeling perfusion MRI. Psychiatry Res. 194, 64–72.
Raichle, M.E., 1998. Behind the scenes of functional brain imaging: a historical and physiological perspective. Proc. Natl. Acad. Sci. USA 95, 765–772.
Raij, T.T., Riekki, T.J., 2012. Poor supplementary motor area activation differentiates auditory verbal hallucination from imagining the hallucination. Neuroimage Clin. 1, 75–80.
Rubinov, M., Sporns, O., 2010. Complex network measures of brain connectivity: uses and interpretations. Neuroimage 52, 1059–1069.
Scheef, L., Manka, C., Daamen, M., Kuhn, K.U., Maier, W., Schild, H.H., Jessen, F., 2010. Resting-state perfusion in nonmedicated schizophrenic patients: a continuous arterial spin-labeling 3.0-T MR study. Radiology 256, 253–260.
Seok, J.H., Park, H.J., Chun, J.W., Lee, S.K., Cho, H.S., Kwon, J.S., Kim, J.J., 2007. White matter abnormalities associated with auditory hallucinations in schizophrenia: a combined study of voxel-based analyses of diffusion tensor imaging and structural magnetic resonance imaging. Psychiatry Res. 156, 93–104.
Shergill, S.S., Murray, R.M., McGuire, P.K., 1998. Auditory hallucinations: a review of psychological treatments. Schizophr. Res. 32, 137–150.
Shin, S.E., Lee, J.S., Kang, M.H., Kim, C.E., Bae, J.N., Jung, G., 2005. Segmented volumes of cerebrum and cerebellum in first episode schizophrenia with auditory hallucinations. Psychiatry Res. 138, 33–42.
Sommer, I.E., Clos, M., Meijering, A.L., Diederen, K.M., Eickhoff, S.B., 2012. Resting state functional connectivity in patients with chronic hallucinations. PLoS One 7, e43516.
Stephane, M., Barton, S., Boutros, N.N., 2001. Auditory verbal hallucinations and dysfunction of the neural substrates of speech. Schizophr. Res. 50, 61–78.
Tremblay, S., Shiller, D.M., Ostry, D.J., 2003. Somatosensory basis of speech production. Nature 423, 866–869.
Tzourio-Mazoyer, N., Landeau, B., Papathanassiou, D., Crivello, F., Etard, O., Delcroix, N., Mazoyer, B., Joliot, M., 2002. Automated anatomical labeling of activations in SPM using a macroscopic anatomical parcellation of the MNI MRI single-subject brain. Neuroimage 15, 273–289.
Upthegrove, R., Broome, M.R., Caldwell, K., Ives, J., Oyebode, F., Wood, S.J., 2016. Understanding auditory verbal hallucinations: a systematic review of current evidence. Acta Psychiatr. Scand. 133, 352–367.
Van Dijk, K.R., Sabuncu, M.R., Buckner, R.L., 2012. The influence of head motion on intrinsic functional connectivity MRI. Neuroimage 59, 431–438.
Wang, Z., 2012. Improving cerebral blood flow quantification for arterial spin labeled perfusion MRI by removing residual motion artifacts and global signal fluctuations. Magn. Reson Imaging 30, 1409–1415.
Wang, Z., Aguirre, G.K., Rao, H., Wang, J., Fernandez-Seara, M.A., Childress, A.R., Detre, J.A., 2008. Empirical optimization of ASL data analysis using an ASL data processing toolbox: asltbx. Magn. Reson Imaging 26, 261–269.
Watts, D.J., Strogatz, S.H., 1998. Collective dynamics of 'small-world' networks. Nature 393, 440–442.
Whiteford, H.A., Degenhardt, L., Rehm, J., Baxter, A.J., Ferrari, A.J., Erskine, H.E., Charlson, F.J., Norman, R.E., Flaxman, A.D., Johns, N., Burstein, R., Murray, C.J., Vos, T., 2013. Global burden of disease attributable to mental and substance use disorders: findings from the Global Burden of Disease study 2010. Lancet 382, 1575–1586.
Zeng, L.L., Shen, H., Liu, L., Hu, D., 2014a. Unsupervised classification of major depression using functional connectivity MRI. Hum. Brain Mapp. 35, 1630–1641.
Zeng, L.L., Wang, D., Fox, M.D., Sabuncu, M., Hu, D., Ge, M., Buckner, R.L., Liu, H., 2014b. Neurobiological basis of head motion in brain imaging. Proc. Natl. Acad. Sci. USA 111, 6058–6062.
Zhu, J., Zhuo, C., Qin, W., Xu, Y., Xu, L., Liu, X., Yu, C., 2015. Altered resting-state cerebral blood flow and its connectivity in schizophrenia. J. Psychiatr. Res. 63, 28–35.
Zhu, Y., Feng, Z., Xu, J., Fu, C., Sun, J., Yang, X., Shi, D., Qin, W., 2016. Increased interhemispheric resting-state functional connectivity after sleep deprivation: a resting-state fMRI study. Brain Imaging Behav. 10, 911–919.